Assessing Yongbyon Reactor Operations Using Landsat Thermal Infrared Satellite Imagery: Challenges and Limitations

Gayeon Ha, Yuji Jeong, Byungmarn Koh *
Korea Institute of Nuclear Nonproliferation and Control, Division of Nuclear Nonproliferation Policy
**Corresponding author: marn@kinac.re.kr*

***Keywords :** Yongbyon, Thermal Infrared Satellite Imagery, Temperature Estimation

1. Introduction

Water discharge was first observed from the Experimental Light Water Reactor (ELWR) at the Yongbyon nuclear complex in North Korea starting in October 2023. It is generally difficult to directly confirm the operational status of North Korean reactors, so indirect estimations are often made by observing water discharges, steam, and movement of specific vehicles using optical imagery. Since the construction phase of the ELWR, the connections between the reactor and piping have been analyzed through images, identifying two water discharge outlets about 200 meters south of the reactor building. The upper outlet is presumed to release emergency cooling water, while the lower outlet releases core cooling water. The International Atomic Energy Agency (IAEA) observed water discharge and steam from the lower outlet through optical images taken in winter and identified warm discharge water using Thermal Infrared (TIR) satellite imagery, suggesting that the reactor might be in commissioning. Thus, the operational status of the reactor can be inferred from the presence of discharges, and the operational stage of the reactor can be estimated from the relatively high temperature of the water discharge. TIR satellite imagery can be used as a supplementary means to optical imagery for temperature estimation of the points of interest.

In this study, we applied four representative temperature estimation techniques to Landsat TIR satellite images from the United States Geological Survey (USGS) to estimate the intake and outflow temperatures and the temperature differences between them, and finally analyzed their limitations.

2. Methodologies

2.1 Data Selection

In this study, Landsat 8 and 9 TIR images of the Yongbyon area were used. These images are freely downloadable from the USGS website (https://earthexplorer.usgs.gov) with an actual spatial resolution of 100 meters, resampled to 30 meters. To consider the seasonal effects of the Kuryong River, we selected five images taken in April and May between 2022 and 2024 (Table 2). To improve the accuracy of temperature estimation, images covered by clouds were excluded. Additionally, optical satellite images from the same dates were used to attempt to confirm the correlation between water discharge presence and estimated temperature differences. However, optical images for April 6, 2024, were unavailable, so water discharge status was estimated based on discharge history near that period.

Table 1: Landsat 8, 9 TIR Specifications

	Landsat 8, 9 TIR
Wavelength	Band 10 (10.60-11.19μm), Band 11 (11.50-12.51μm)
Spatial Resolution	100m (resampled to 30m)
Temporal Resolution	8 days (each 16 days)
Data Source	USGS

Table 2: Satellite Imagery and Related Information

		2022.4.1.	**2023.4.12.**	**2024.4.6.**	**2024.4.30.**	**2024.5.16.**
Area		Yongbyon	Yongbyon	Yongbyon	Yongbyon	Yongbyon
Temp (℃) / Humidity (%)		10 / 48	11 / 48	15 / 41	18 / 51	17 / 51
Thermal Infrared Imagery		Landsat 9	Landsat 8	Landsat 9	Landsat 8	Landsat 8
		11:16 AM KST	11:15 AM KST	11:16 AM KST	11:15 AM KST	11:15 AM KST
Optical Imagery		WorldView-1	GeoEye-1	N/A	GeoEye-1	GeoEye-1
		2:48 PM KST	11:29 AM KST		11:28 AM KST	11:08 AM KST
ㄴ	**Water Discharge**	X	X	X (estimated)	O	O

2.2 Selection of Points of Interest

High-resolution optical satellite images were used to select temperature estimation points. By overlaying Landsat TIR images with high-resolution optical images (approximately 0.5m resolution), the intake and outflow points of the ELWR were identified, and three consecutive pixels each were selected near the intake and outflow based on the TIR images (Figure 1). It is important to note that there is a limitation due to the positional uncertainty caused by the difficulty of relative geometric correction between optical and TIR images.

Using the temperature estimation techniques discussed in Section 2.3, the temperature for each pixel can be estimated, and the average of the three consecutive pixels at the intake and outflow are defined as the ELWR intake temperature (#1) and outflow temperature (#2), respectively. Therefore, the temperature difference of the water intake and outflow is calculated as the difference between these two temperatures (#2 - #1). All calculations, including the application of temperature estimation techniques, were performed using Python-based self-written code and the open-source GIS (Information System) software, QGIS (Quantum GIS).

2.3 Temperature Estimation

Temperature estimation using TIR sensors is based on emitted radiative energy, which differs from the actual temperature due to surface emissivity and atmospheric effects. In this study, four representative temperature estimation techniques for Landsat TIR identified through previous studies were utilized (Table 3) [1]: Brightness Temperature (BT), Mono-window (MW), Single-channel (SC), and Split-window (SW). The methods differ in how they assume and correct for atmospheric effects and emissivity, with the following accuracy: BT (± 6.00 ℃) < MW (± 2.41 ℃) < SC (± 1.31 ℃) < SW (± 1.10 ℃). The calculation formulas for each technique are omitted in this paper.

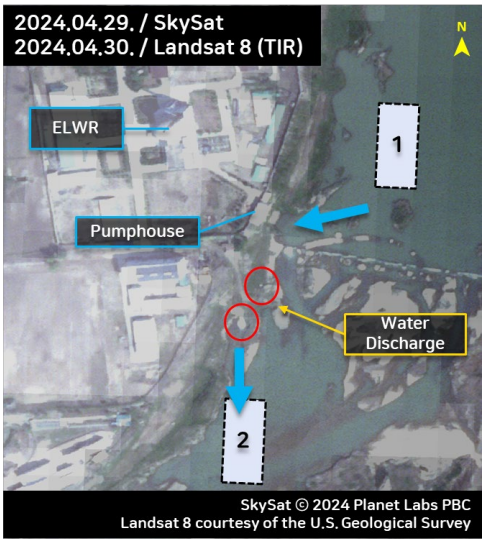

Figure 1: Selection of Points of interest

3. Results

First, the intake and outflow temperatures of the reactor were estimated using the four temperature estimation techniques. Figure 2 shows the temperature estimation results for the day when discharge was observed (May 16, 2024). Significant differences in estimated temperatures were observed depending on the methodology (up to 3.2℃ at the intake and 3.9℃ at the outflow). The key point here is the estimation accuracy of the methodologies. While SW has an accuracy range of approximately ±1.1℃, BT is known to have a maximum accuracy of ±6.0℃. Therefore, the temperature difference between the intake and outflow was calculated using the SW technique with the smallest estimation error. The results of the temperature difference estimation for the five images are shown in Figure 3. It is practically impossible to compare these results with the actual temperature differences, so this study aimed to confirm the relationship between observed discharge and temperature differences.

Table 3: Representative Temperature Estimation Methods Using Landsat TIR

Method	Characteristics	Assumptions		Accuracy (Approx.)	Source
		Emissivity	Atmospheric Influence		
Brightness Temperature (BT)	The Simplest calculation	No (Assumes 1)	No	± 6.00 ℃	[2]
Mono-window Algorithm (MW)	Uses a single band	Yes	Yes	± 2.41 ℃	[3]
Single-channel Algorithm (SC)	Uses a single band	Yes	Yes	± 1.31 ℃	[4]
Split-window Algorithm (SW)	Uses two thermal infrared bands	Yes	Yes	± 1.10 ℃	[5]

On days when discharge was not observed (blue points), the temperature differences ranged from +0.45 to 1.40℃. On days when discharge was observed (yellow points), the temperature differences ranged from +2.19 to 2.79℃. Although more data is needed for further validation, it was confirmed that the temperature differences are relatively large when discharge occurs. However, it should be noted that if the estimated temperature differences fall within the estimation accuracy range (±2.2℃), their significance may be lost.

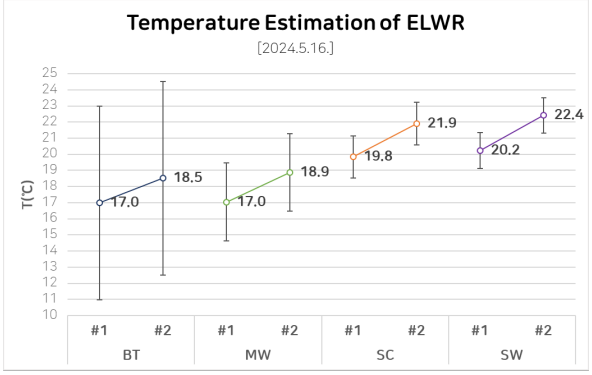

Figure 2: Comparison of ELWR Intake and Outflow Temperatures by Estimation Methods (2024.5.16.)

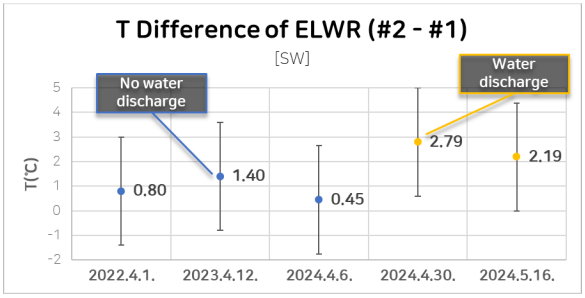

Figure 3: Comparison of ELWR Intake and Outflow Temperature Differences Using SW Method

4. Limitations

As discussed above, there are several limitations in this study. First, the low resolution of Landsat TIR (30m) makes it difficult to accurately select points of interest. This can be affected by buildings or riverbank terrain. Despite selecting points based on high-resolution optical images, positional errors occur due to the lack of relative geometric correction with TIR. Second, seasonal changes in the Kuryong River's condition can affect the river's water level, exposing the riverbed or covering it with snow and ice in winter (Figure 4). These changes can affect not only the selection of points of interest but also the temperature estimation. Third, the temperature estimation techniques themselves have errors. If the estimated temperature difference falls within the accuracy range, its significance may be lost. These limitations should be considered when interpreting the study results.

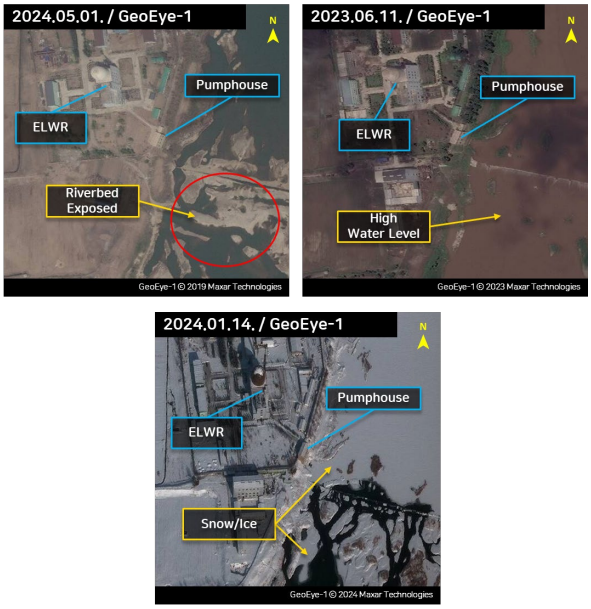

Figure 4: Seasonal Surface Condition Changes of the Kuryong River

5. Conclusions

This study is significant in applying representative temperature estimation methods using Landsat TIR to estimate the temperature differences of reactor discharge at the Kuryong River and discuss their limitations. Although a correlation between water discharge and temperature differences was confirmed with a few images, many limitations were identified, including the resolution and accuracy of the estimation methods. Further validation with more data is needed, and using higher-resolution thermal infrared sensors may overcome some of the aforementioned limitations. Additionally, integrating additional data sources such as high-resolution optical images can improve reactor operation monitoring accuracy.

REFERENCES

[1] G. Ha, M. Kim, J. Han, Application and Comparison of Converting Temperature from Thermal Infrared Satellite Imagery for Nuclear Activity Detection and Monitoring, NSTAR-23PS52-306, 2023.
[2] Landsat 8 Data Users Handbook, USGS, version 5.0, 2019.
[3] Z. Qin, A. Karnieli, P. Berliner, A Mono-window Algorithm for Retrieving Land Surface Temperature from Landsat TM Data and its Application to the Israel-Egypt Border Region, International Journal of Remote Sensing, 22(18), pp.3719-3746, 2001.
[4] J. C. Jimenez-Munoz, J. A. Sobrino, A Generalized Single-channel Method for Retrieving Land Surface Temperature from Remote Sensing Data, Journal of Geophysical Research, 108(22), 2003.
[5] L. M. McMillin, Estimation of Sea Surface Temperatures from Two Infrared Window Measurements with Different Absorption, Journal of Geophysical Research, 80(36), pp.5113-5117, 1975.